A new method for determining the transfer function of an Acousto optical tunable filter

A. Mahieux,[*,1] V. Wilquet,[1] R. Drummond,[1]
D. Belyaev,[2] A. Federova,[2] and A.C. Vandaele[1]

[1]*Belgian Institute for Space Aeronomy, 3 av. Circulaire, B-1180 Brussels, Belgium.*
[2]*Space Research Institute (IKI), 84/32 Profsoyuznaya Str., 117997, Moscow, Russia.*
** Corresponding author: arnaud.mahieux@aeronomie.be*

Abstract: The current study describes the determination of the transfer function of an Acousto Optical Tunable Filter from the in-flight solar observations of the SOIR instrument on board Venus Express. An approach is proposed in order to reconstruct the transfer function profile from the analysis of various solar lines. Moreover this technique allows the determination of the evolution of the transfer function as a function of the AOTF radio frequency.

OCIS codes: (070.1060) Acousto-optical signal processing; (300.1030) Absorption

References and links

1. D. Nevejans, E. Neefs, E. Van Ransbeeck, S. Berkenbosch, R. Clairquin, L. De Vos, W. Moelans, S. Glorieux, A. Baeke, O. Korablev, I. Vinogradov, Y. Kalinnikov, B. Bach, J.-P. Dubois, and E. Villard, "Compact high-resolution space-borne echelle grating spectrometer with AOTF based on order sorting for the infrared domain from 2.2 to 4.3 micrometer," Appl. Opt. **45**, 5191-5206 (2006).
2. A. Mahieux, S. Berkenbosch, R. Clairquin, D. Fussen, N. Mateshvili, E. Neefs, D. Nevejans, B. Ristic, A. C. Vandaele, V. Wilquet, D. Belyaev, A. Fedorova, O. Korablev, E. Villard, F. Montmessin, and J.-L. Bertaux, "In-Flight performance and calibration of SPICAV SOIR on board Venus Express," Appl. Opt. **47**, 2252-65 (2008).
3. J. L. Bertaux, D. Nevejans, O. Korablev, E. Villard, E. Quémerais, E. Neefs, F. Montmessin, F. Leblanc, J. P. Dubois, and E. Dimarellis, "SPICAV on Venus Express: Three spectrometers to study the global structure and composition of the Venus atmosphere," Planet. Space Sci. **55**, 1673-1700 (2007).
4. D. V. Titov and e. al., "Venus Express science planning," Planetary and Space Science **54**, 1279-1297 (2006).
5. D. A. Glenar, J. J. Hillman, B. Saif, and J. Bergstralh, "Acousto-optic imaging spectropolarimetry for remote sensing," Appl. Opt. **33**, 7412-7424 (1994).
6. J. Xu and R. Stroud, "Acousto-Optic devices," John Wiley & Sons, Inc., New-York, 1992.
7. A. C. Vandaele, M. De Mazière, R. Drummond, A. Mahieux, E. Neefs, V. Wilquet, D. Belyaev, A. Fedorova, O. Korablev, F. Montmessin, and J.-L. Bertaux, "Composition of the Venus mesosphere measured by SOIR on board Venus Express," J. Geophysic. Res., doi:10.1029/2008JE003140 (2008).
8. M. S. Gottlieb, "Acousto-optical Tunable filter," in *Design and fabrication of acousto-optic devices*, A. P. Goutzoulis, D. R. Pape and S. V. Kulakov, eds., pp. 197-283, Marcel Dekker, New-York (1994).
9. F. Hase, P. Demoulin, A. J. Sauval, G. C. Toon, P. F. Bernath, A. Goldman, J. W. Hannigan, and C. P. Rinsland, "An empirical line-by-line model for the infrared solar transmittance spectrum from 700 to 5000 cm^{-1}," J. Quant. Spectrosc. Radiat. Transfer **102**, 450-463 (2006).

1. Introduction

This study has been motivated by the fact that our team is involved in the analysis of the data of the SOIR instrument on Venus Express. SOIR [1,2] (Solar Occultation in the InfraRed) is an infrared spectrometer mounted on top of the SPICAV [3] instrument on board Venus Express [4]. The optics includes an echelle grating, used for splitting the light into 94 useful diffraction orders. The diffraction order selection is performed using an Acousto Optical Tunable Filter (AOTF) located between the entrance optics and the grating. The radio

#104035 - $15.00 USD Received 13 Nov 2008; revised 22 Dec 2008; accepted 1 Jan 2009; published 30 Jan 2009

transducer of the AOTF is electrically commanded, and its frequency varies from 12700 kHz to 26325 kHz. In terms of wavelength, it corresponds to the 2.2 - 4.3 µm region.

The AOTF physical characteristics have been extensively described elsewhere [1,2] and will be only briefly summarized here. Theoretically, the AOTF transfer function may be modelled as a sinc^2 function [5,6]. However, data processing demonstrated that a sinc^2 function does not correctly reproduce the AOTF function [7].

Due to short construction time, the AOTF transfer function could not be measured correctly throughout its whole wavenumber range in the laboratory before launch. Moreover, it is suspected that the AOTF crystal suffered some damage during take off, which probably changed the shape of the transfer function. A new method has been derived to determine the transfer function of the AOTF using only in-flight measurements, i.e. direct Sun measurements. This new method is described and illustrated in the present study.

Section 2 gives a short description of the optics of the SOIR instrument, and explains how it can be modelled. The method used to retrieve the AOTF transfer function is reported in Section 3, and results are presented in Section 4. Finally, conclusions are drawn in Section 5.

2. The SOIR instrument

2.1. Description

During a measurement, a diffraction order is selected for study based on spectroscopic consideration. The AOTF radiofrequency is tuned in accordance, so that the maximum of transmission of the filter corresponds to the selected wavelength, which most of the time corresponds to the central wavelength of the chosen order. An AOTF frequency to wavenumber relationship has been defined in [2]. Hereafter the selected order will be called central order or simply order.

After passing through the entrance optics (aperture followed by elements 1 and 2 of Fig. 1), light enters the AOTF (elements 3 of Fig. 1). This component filters the light by a given function, namely the AOTF transfer function, which has to be determined. The light is then diffracted by the echelle grating (element 7 of Fig. 1) and finally it is recorded by the detector (elements 10 of Fig. 1).

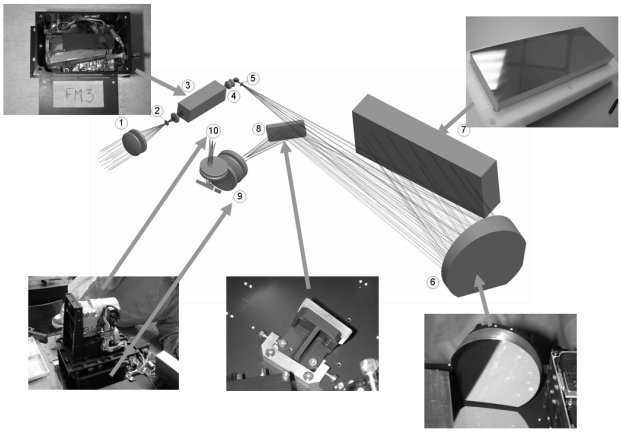

Fig. 1. SOIR optics. The AOTF (3) is located after the entrance optics (1 and 2). The echelle grating (7) diffracts the incoming light, which is recorded by the detector (10).

The free spectral range (FSR) of the echelle spectrometer, i.e. the spectral interval in which there is no interference or superposition of light from adjacent orders equals 22.38 cm^{-1}, whereas the bandwidth of the AOTF was originally designed to be 20 cm^{-1}, as measured on ground before launch [1] . The real measured bandwidth of SOIR is ~24 cm^{-1}, creating some order leakage on the detector [2]. The contribution coming from the non central orders is

#104035 - $15.00 USD Received 13 Nov 2008; revised 22 Dec 2008; accepted 1 Jan 2009; published 30 Jan 2009

certainly not negligible and has to be taken into account. In general, we consider a total of 7 contributing orders to determine the final signal on the detector, as it is the best compromise between calculation speed and accuracy of the retrieved spectra [2,7]. In some cases, for example when analysing the deep CO_2 lines present in the orders 103 to 112, a total of 9 orders is used.

2.2. Procedure to reconstruct a SOIR spectrum

To simulate these steps, the following procedure is applied. First the theoretical transmittance spectrum is convolved by the instrumental function, modelled by a sinc² function as described in [2], whose width corresponds to the achieved resolution of the instrument, i.e. 0.15 cm^{-1} (Panels A and B of Fig. 2). Next, it is multiplied by the AOTF transfer function (Panel C of Fig. 2). And finally the order addition is performed (Panels D and E of Fig. 2). For this operation, three orders with a higher diffraction number and three orders with a lower diffraction number compared to the central order are taken into account, giving a total of 7 orders.

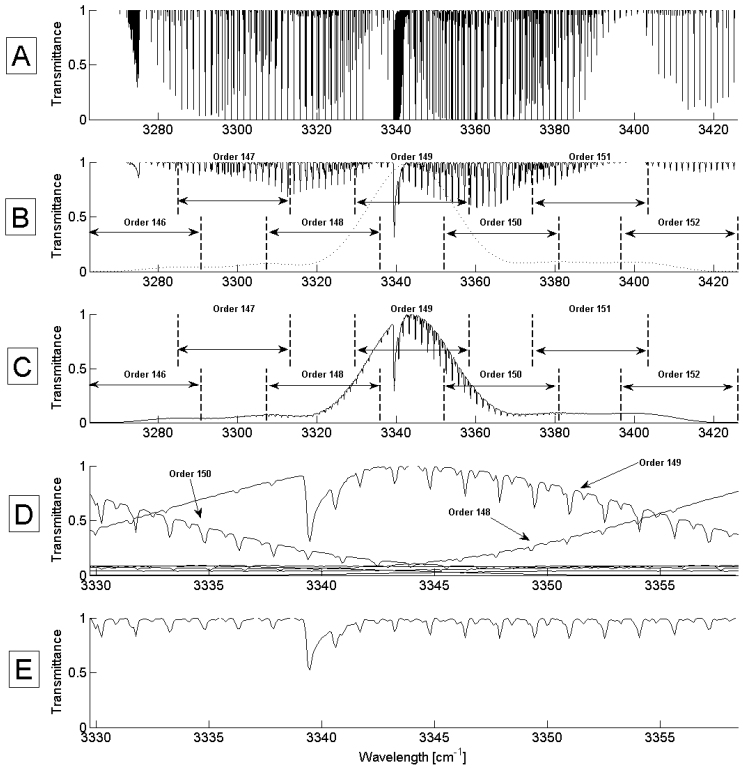

Fig. 2. SOIR spectrum construction process. Panel A depicts the CO_2 absorption lines at 2.99 µm (corresponding to diffraction order 149) at a very high resolution. Panel B shows the CO_2 absorption lines convolved by the instrument function. The dotted line is the AOTF transfer function for the diffraction order 149. The vertical dashed lines between the arrows show the limits of each diffraction order. Panel C depicts the spectrum after multiplication by the AOTF transfer function, i.e. what reaches the echelle grating in terms of transmittance. Panel D shows the contribution of each diffracted spectrum after the echelle grating. The orders 146, 147, 151 and 152 have small contributions, but may not be neglected. Finally, the simulated transmittance is represented in panel E, and is the sum of all diffracted orders contributions.

The signal is read across 32 rows of pixels on the detector of SOIR [2]. Some telemetric constraints force us to sum these rows into several groups, or bins. Four different binning cases, have been defined and used [2]: 2 bins of 16 rows (binning 2x16), 2 bins of 12 rows

#104035 - $15.00 USD Received 13 Nov 2008; revised 22 Dec 2008; accepted 1 Jan 2009; published 30 Jan 2009

(binning 2x12), 8 bins of 4 rows (binning 8x4) and 4 bins of 4 rows (binning 4x4). As an example, 'binning 2x16' means that 2 spectra are recorded simultaneously, the first one corresponds to the signal received on rows 1 to 16 and the second one to the signal on rows 17 to 32.

2.3. Propagation of light through the SOIR crystal

If we consider that the light travels as planar waves through the AOTF crystal, the transfer function can be modelled fairly well by a single sinc^2 function [8]. However, after launch of the VEX spacecraft, it was realized that the width of AOTF transfer function had changed and that the side lobes of the function were different to what had been measured on Earth [2]. We interpret this change as the result of some damage suffered by the device during the take off phase. Because of this probable slight damage of the AOTF crystal, one could consider the medium is no longer perfectly homogeneous. The light would no longer travel as a planar wave. There are two consequences to this: (1) The light at the output is the result of several planar waves propagating through the crystal; and (2) the transmission through the crystal will depend on the physical portion of the medium which is passed through. The bandpass function will then (1) be modelled as the sum of several sinc^2 functions and (2) depends on the position of the detector rows, therefore on the binning case. Moreover, it should be noted that the AOTF function depends on the radio frequency applied to the device, and therefore on the wavelength of the light transmitted through the crystal.

3. Method for reconstituting the AOTF transfer function

3.1. Measurement description

A dedicated operation mode of SOIR is used to obtain the AOTF transfer function, namely the miniscan mode [2]. A miniscan consists of varying the AOTF frequency by small steps, i.e. 1, 5 or 20 kHz, while looking at the Sun from orbit directly, without intersecting the planet's atmosphere. It offers the possibility of measuring the Fraunhofer solar absorption lines [9] precisely. These lines being clearly known and very sharp (sharper than the instrument function [2]), one can deduce the shape of the AOTF transfer function.

The miniscans cover wavenumber regions spanning a minimum of 68.7 cm^{-1}, a maximum of 157.3 cm^{-1} with an average value of 81.0 cm^{-1}.

As explained in the previous section, the absorption lines from three orders with a higher diffraction number and three orders with a lower diffraction number compared to the central order can have a significant contribution to the measured spectrum. The solar absorption lines used for the current study have been carefully chosen in such a way that no line from any of the -3 to +3 adjacent orders falls on the same pixel nor on nearby pixels of the detector. This is easily performed knowing the relation diffraction order – wavenumber, which allows the accurate determination of the pixel number on which each solar line falls. The solar absorption lines studied have also a minimum of 0.92 in transmittance. The solar lines have also been chosen such that they cover the entire spectral range sounded by the instrument, as the AOTF bandpass function depends on the central wavelength. The pixel to pixel variation and the detector sensitivity variation have been removed as explained in [2].

3.2. Procedure

In the following we will distinguish between a local and a global model. The local model allows the definition of the parameters needed to construct the AOTF bandpass function from a given solar line, i.e. corresponding to a given central wavenumber. This is repeated as many times as the number of selected solar lines. The global model is then used to draw trends in the fitted parameters in function of wavenumber, so that the AOTF bandpass function can be built for any given central wavenumber.

#104035 - $15.00 USD Received 13 Nov 2008; revised 22 Dec 2008; accepted 1 Jan 2009; published 30 Jan 2009

3.3. Local model: AOTF transfer function model

The model that will be used to fit the AOTF transfer function is a sum of 5 sinc² functions:

$$AOTF\left(wn\right)=\sum_{i=-2}^{2}\max\left(0,I_i\right)\cdot\mathrm{sinc}^2\left[0.886\cdot\frac{\left(wn-wn_{0i}\right)}{fwhm_i}\right] \quad (1)$$

where wn is the wavenumber, I_i are the intensity coefficients, wn_{0i} the relative wavenumber position of the maximum of the sinc² functions, and $fwhm_i$ the full width half max of each sinc² function. It results in 14 variables to fit, as the first relative wavenumber wn_{00} has to be equal to zero, i.e. centred on the maximum.

A decision had to be made on the number of sinc² functions to use. This number had to be odd, as the number of sinc² had to be the same on both sides of the central sinc². It turned out that 7 cannot be used, because no reliable information can be obtained so far away from the AOTF maximum, as the miniscans that we used for this work do not cover that region. 5 sinc² is the maximum number that could be used.

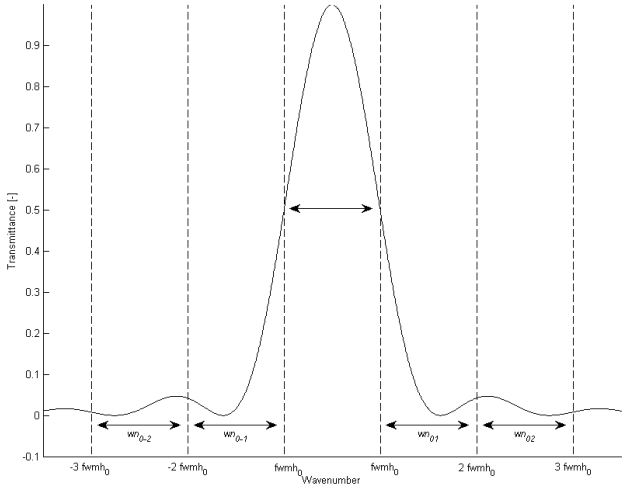

Fig. 3. Definition of the interval variation of the wn_{0i}. This is a plot of one sinc² function (the one noted '0') to show how the position of the wn_{0i} is constrained using the value of $fwhm_0$. The width of the arrows equals to $fwhm_0$.

These parameters are fitted for each observed solar absorption line selected above using a Simplex algorithm. Constraints are also defined: all the I_i and $fwhm_i$ values have to be positive – even after convergence; the values of the wn_{0i} must remain in well distinct intervals, defined as multiples of $fwhm_0$, as illustrated in Fig. 3.

As stated in Section 3.1, the average wavenumber width of the miniscans is 81 cm^{-1}. The value of $fwhm_0$ is around 24 cm^{-1} [2]. As the miniscans are not always centred on the solar line, up to three AOTF transfer function intervals may be measured using one solar line. Therefore, using several measurements of one line, one can reconstruct a maximum of 5 intervals. The inner three intervals are very well defined, and the outer two are less certain.

As stated in Section 3.1, the fit is performed on a set of measurements of each solar line, and for each measurement the pixel to pixel variation as well as the detector sensitivity variation is tentatively removed. The residual background is modelled for each measurement by a linear function, which may differ from miniscan to miniscan. For each measurement j, the model becomes:

#104035 - $15.00 USD Received 13 Nov 2008; revised 22 Dec 2008; accepted 1 Jan 2009; published 30 Jan 2009

$$AOTF_j(wn) = \underbrace{\sum_{i=-2}^{2} \max(0, I_i)\,\mathrm{sinc}^2\left[0.886 \cdot \frac{(wn - wn_{0i})}{fwhm_i}\right]}_{AOTF(wn)} + \alpha_j \cdot wn + \beta_j \qquad (2)$$

where α_j and β_j are the coefficients of the background of the measurement j, and the I_i, wn_{0i} and $fwhm_i$ are the coefficients common to each measurement of the same line.

3.4. Global model: Variation of the local AOTF transfer function model with wavenumber

The local model defined in the above section can be performed for all the selected solar absorption lines throughout the whole SOIR spectral range, i.e. from 2250 to 4370 cm^{-1}. However, each separate local model is assumed to be related to the other ones, because the evolution of the bandpass function with wavenumber is smooth (see Fig. 7). We have supposed that the 14 parameters were varying linearly across the SOIR spectral range.

$$X = a_X \cdot wn + b_X \qquad (3)$$

where X is one of the 14 parameters defining the AOTF function (I_i, $wn_{0i(\neq 0)}$ or $fwhm_i$), a_X the linear coefficient and b_X the constant coefficient.

Finally, a set of 28 coefficients has to be fitted. This fit is also performed using a Simplex algorithm, but with no constraints.

3.5. Interaction between the global and local models

The local models are all driven by the global model. They each receive a set of 14 initial variables obtained from the linear regression of the global model at the wavenumber of the solar absorption line, i.e. the absolute wavenumber of the maximum of the central sinc² function. Each local model returns a fitted set of the 14 variables, which are used by the global model for fitting its 28 variables a_X and b_X. The interaction between the global and the local model is presented in Fig. 4.

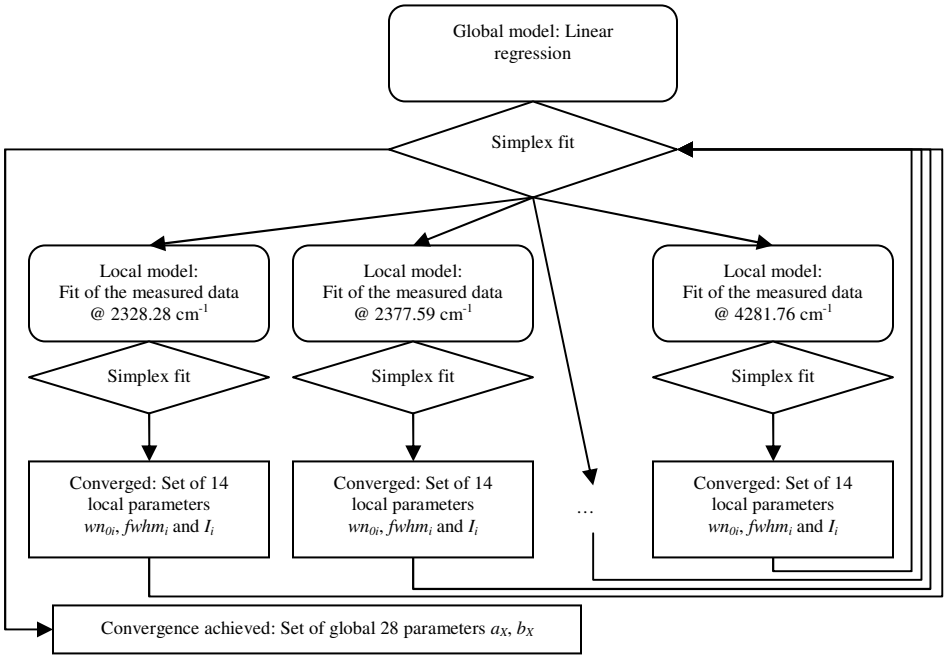

Fig. 4. Description of the interaction between the global model and the local model

#104035 - $15.00 USD Received 13 Nov 2008; revised 22 Dec 2008; accepted 1 Jan 2009; published 30 Jan 2009

The set of 28 parameters a_X and b_X, where X may be *FWMH*, *I* or wn_0, is obtained when convergence is achieved. Figure 5 shows the convergence of parameters a_{FWMH_0} and b_{FWMH_0} as well as a_{I_1} and b_{I_1} of bin 1 in the binning 2x12 case, as well as the convergence of the fit residuals of the global model.

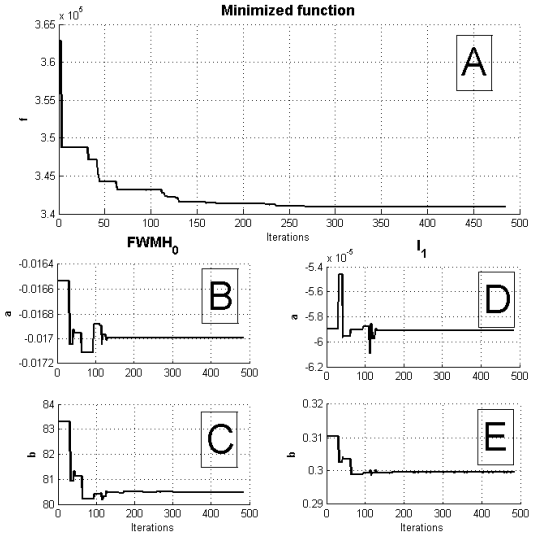

Fig. 5. Convergence of the global model for bin 1 of binning 2x12. The convergence occurred after 482 steps. Panel A shows the convergence of the function minimized by the Simplex algorithm. Panels B and C show the convergence of parameters a_{FWMH_0} and b_{FWMH_0}, and panels D and E concern the convergence of a_{I_1} and b_{I_1}.

4. Results

The method described in Section 3 has been applied to the observations performed between September 10th 2006 (orbit 142) and March 3rd 2008 (orbit 682) during 30 different miniscans. The retrievals have been performed for all the binning cases defined in Section 2. Figure 6 shows the local fit for the 2328.28 cm^{-1} solar line. Similar fits have been obtained for all the 30 solar lines scanned.

#104035 - $15.00 USD Received 13 Nov 2008; revised 22 Dec 2008; accepted 1 Jan 2009; published 30 Jan 2009

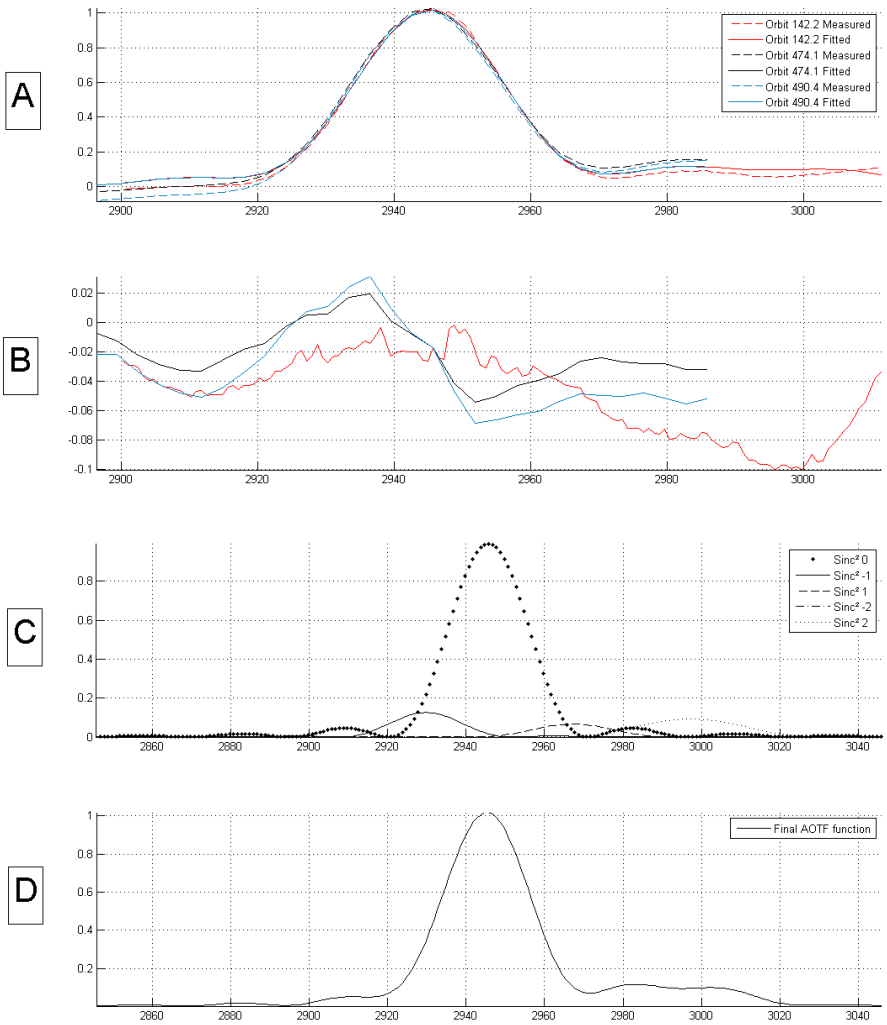

Fig. 6. Fit of the 2943.70 cm^{-1} solar line. Panel A shows the fit of the solar line at 2943.70 cm^{-1} solar line. This line has been scanned three times, during orbits 142.2 (20060910), 474.1 (20070808) and 490.1 (20070824). The measured AOTF transfer functions are plotted as solid lines; the fitted functions are plotted as dashed lines. They depict the models described in Eq. 2. Panel B shows the residuals of the fit of the three solar lines. Panel C shows the 5 $sinc^2$ functions, and panel D shows the final AOTF transfer function, obtained from the model described in Eq. (1).

It has to be noted that the AOTF transfer function obtained using this technique is the mirror of the one that has to be used for spectra analyses. This finds its explanation in the miniscan measurement scheme. The solar line may be considered as a Dirac peak. It is scanned while slightly incrementing the AOTF frequency value, i.e. while moving the physical AOTF functions along the wavenumber axis to the right. As the source remains fixed, and the recorder shifts in terms of wavenumber, what we record is the opposite of the AOTF transfer function.

#104035 - $15.00 USD Received 13 Nov 2008; revised 22 Dec 2008; accepted 1 Jan 2009; published 30 Jan 2009

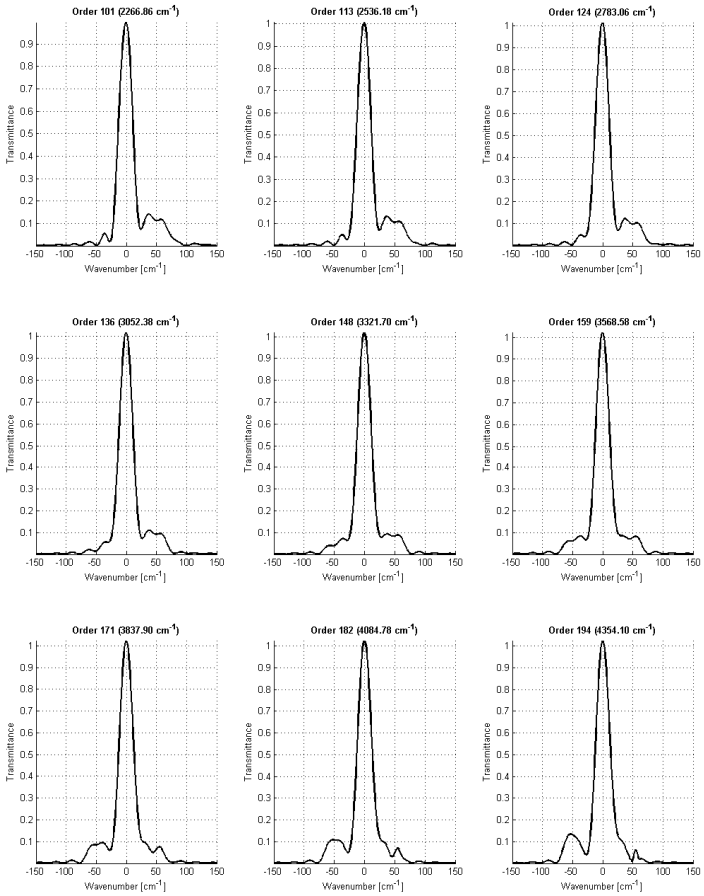

Fig. 7. AOTF final functions retrieved for bin 1 (binning 2x12) for several orders.

If one could displace the solar line, we would obtain directly the AOTF transfer function. The AOTF transfer functions obtained are shown in Fig. 7 for bin 1, in the 2x12 binning case. An example of coefficients set is given in Table 1. To obtain the coefficients sets of other binning cases, please contact the corresponding author.

Table 1: Example of coefficients set of the AOTF transfer function fit for bin 2 of the binning cases 2x16.

a_{fwhm00}	1.620E-3	$a_{wn0\text{-}1}$	-2.877E-3	$a_{I0\text{-}0}$	0
b_{fwhm00}	1.780E1	$b_{wn0\text{-}1}$	-7.281E0	$b_{I0\text{-}0}$	1
$a_{fwhm0\text{-}1}$	4.813E-3	a_{wn01}	2.574E-3	$a_{I0\text{-}1}$	-1.145E-5
$b_{fwhm0\text{-}1}$	8.476E0	b_{wn01}	1.348E1	$b_{I0\text{-}1}$	1.267E-1
a_{fwhm01}	-2.046E-3	$a_{wn0\text{-}2}$	-6.597E-3	a_{I01}	-3.440E-5
b_{fwhm01}	3.345E1	$b_{wn0\text{-}2}$	-3.358E1	b_{I01}	1.950E-1
$a_{fwhm0\text{-}2}$	5.314E-3	a_{wn02}	2.619E-4	$a_{I0\text{-}2}$	4.641E-5
$b_{fwhm0\text{-}2}$	2.214E0	b_{wn02}	4.811E1	$b_{I0\text{-}2}$	-6.093E-2
a_{fwhm02}	6.592E-3	a_{I00}	1.936E-5	a_{I02}	-8.524E-5
b_{fwhm02}	1.345E1	b_{I00}	9.246E-1	b_{I02}	3.360E-1

#104035 - $15.00 USD Received 13 Nov 2008; revised 22 Dec 2008; accepted 1 Jan 2009; published 30 Jan 2009

5. Conclusions

The method described in this paper has been used to retrieve the AOTF transfer function of the SOIR instrument on board Venus Express. It was retrieved using 80 in-flight dedicated measurements, called miniscans, while scanning 30 solar lines. The method has been applied to all binning cases used by SOIR, and they all converge, both on the local (for one frequency) and the global scales (for all frequencies). This study has demonstrated that considering only a $sinc^2$ function to represent the AOTF bandpass function is not sufficient, and that at least 5 $sinc^2$ functions have to be introduced to better quantify the relative importance of the side lobes.

In the future, new measurement periods will be devoted to solar miniscans and will provide the possibility to monitor the evolution of the AOTF transfer function in time. This will moreover allow us to follow more accurately the status of the SOIR instrument throughout its mission in space, and more specifically the status of one of its main constituent, the AOTF.

The AOTF function determined in this paper has been used for the analysis of Venus' spectra recorded by SOIR. Although it is not easy to distinguish between different sources of possible disagreement (influence of temperature on some lines, radiative transfer issues, model of the Venus atmosphere), the agreement between simulations and recorded spectra was best when using the new AOTF transfer function. This part will be dealt in a forthcoming paper, as it is beyond the scope of the present one.

#104035 - $15.00 USD Received 13 Nov 2008; revised 22 Dec 2008; accepted 1 Jan 2009; published 30 Jan 2009